




Article

Diesel Governor Tuning for Isolated Hybrid Power Systems

Muhammad Asad ¹, Sergio Martinez ^{2,*} and Jose Angel Sanchez-Fernandez ¹

¹ Department of Hydraulic, Energy and Environmental Engineering, E.T.S.I. Caminos Canales y Puertos, Universidad Politécnica de Madrid, 28040 Madrid, Spain; m.asad@alumnos.upm.es (M.A.); joseangel.sanchez@upm.es (J.A.S.-F.)

² Department of Electrical Engineering, E.T.S.I. Industriales, Universidad Politécnica de Madrid, 28006 Madrid, Spain

* Correspondence: sergio.martinez@upm.es

Abstract: In recent decades, renewable energy sources, such as wind power, have extraordinarily increased their participation in the energy mix throughout the world. This progression has played an important role in lowering the usage of fossil fuels. In addition, it has reduced environmental hazards and increased the emergence of hybrid power systems, mainly in remote areas. In some of these areas, diesel power plants were the only previous source of energy. Irrespective of the benefits, hybrid power systems might face problems such as frequency deviations. To contribute to reducing these problems, this paper presents a methodology to tune diesel engine governors using the Student Psychology-Based Algorithm. This proposed methodology enhances some metrics of controller performance, such as the integral square error, integral absolute error, and number of sign changes in the frequency derivative. This approach has been tested against different perturbations (step, ramp and random). To validate the effectiveness of the proposed approach, it has been simulated in relation to the San Cristobal Island (Ecuador) hybrid wind–diesel power system. The simulation results show that the governor tuned with the proposed approach provides a better system response.

Keywords: diesel engine governor; isolated power system; power-frequency control; wind–diesel power plant



Citation: Asad, M.; Martinez, S.; Sanchez-Fernandez, J.A. Diesel Governor Tuning for Isolated Hybrid Power Systems. *Electronics* **2023**, *12*, 2487. <https://doi.org/10.3390/electronics12112487>

Academic Editor: Jen-Hao Teng

Received: 28 April 2023

Revised: 25 May 2023

Accepted: 30 May 2023

Published: 31 May 2023



Copyright: © 2023 by the authors. Licensee MDPI, Basel, Switzerland. This article is an open access article distributed under the terms and conditions of the Creative Commons Attribution (CC BY) license (<https://creativecommons.org/licenses/by/4.0/>).

1. Introduction

Stand-alone diesel power generation is the major and most adaptive energy source on islands and in remote areas that are isolated, completely or partially, from grid supply [1,2]. In the last few years, these stand-alone power systems have been subject to restrictions imposed by international environmental regulations due to greenhouse gas emissions [3,4]. In addition, the sudden depletion of fossil fuels increased the cost of both diesel and its transportation to these islands and remote areas [5].

To overcome these problems, the integration of renewable energy (RE) with the existing power infrastructure is a commonly used solution. Fortunately, most of these islands and remote areas usually have major potential in terms of renewable energy sources such as wind or solar energy, which are widely distributed, freely available, and environmentally friendly, as compared to conventional fossil fuel-based energy sources [1]. To support this initiative, many developed and developing countries have introduced various strategies, re-developed their policies, and offered subsidies to power regulations [6]. To take advantage of these opportunities, isolated hybrid wind–diesel power system installations have been constructed on islands and in remote areas [7,8]. Some examples of islands in Europe with high RE potential are the Canary Islands [9], Aegean Islands [10], the archipelago of the Flores-Azores [11], etc. Similarly, in Latin America, the Galapagos Islands [12,13], and in the South China Sea, the Yong Shu Island [14]. The major benefits of integrating wind energy sources into remote isolated power systems are not just limited to savings in fuel consumption. Indeed, compared to the traditional diesel system, wind power integration

could offer additional advantages such as providing extra energy to the microgrid, reducing pollution and greenhouse gas emissions, and hedging the risk of unexpected fuel price increases [15].

Despite the above-mentioned advantages, hybrid wind–diesel power systems (WDPSs) might face certain problems, such as power system frequency deviations [16,17], among others. Some examples reported in the literature that show frequency deviation effects on power systems include El Hierro Island (Spain) [7], the Galapagos Islands (Ecuador) [18], remote Arctic regions (Yakutia, Russia) [19], and Dakhla (Morocco) [20]. There are multiple reasons that can cause frequency fluctuations in power systems: load or generation variations, load or generator trips, faults, interactions among controllers, etc. In power systems with a high share of wind energy, one important cause of frequency variations is the fluctuation of the power injected into the grid by wind generators due to wind speed variations. Due to high wind intermittency, the power quality of the system might decrease, especially when the system is characterized by a low inertial response. Despite the rapid development of wind power, wind power consumption and integration into conventional power systems are not optimal [15]. The available power fluctuates with time due to wind variations or is restricted due to environmental conditions. This is why various techniques or methods, such as wind power curtailment, and energy storage systems, such as flywheels, capacitors, batteries, etc., are adopted to overcome these problems. However, the cost of these additional storage systems, in addition to other factors such as environmental restrictions, political influences (variations in government policies), etc., cause hurdles in relation to the further development of this technology. Furthermore, several control techniques were developed to run the power system within its pre-defined protective zone, without the need of any additional installation. Moreover, deviations in power system frequency can endanger the stability and reliability of any power network [21–23]. This is why hybrid WDPSs might face frequency deviations or might be operated at the edge of the lower frequency limit [23].

In [18], a root locus analysis is used to find the controller gain parameters of a diesel governor, which leads to power system frequency regulation. It is a first approach to the problem of governor tuning, although it is far from being optimum. This paper proposes a methodology for optimum tuning of diesel engine governors to enhance power system frequency stability using an exhaustive search approach according to controller quality indices [24,25]. The main advantage of this approach is providing a unique optimum combination of controller gain parameters.

This paper is organized as follows. Section 2 briefly explains the diesel governor model implemented in this research work and its characteristics. In Section 3, a comprehensive discussion of the proposed methodology, which is based on the Student Psychology-Based Algorithm (SPBA), is presented. Furthermore, a detailed case study is explained in Section 4. In Section 5, the simulation results are discussed. Finally, conclusions are presented in Section 6.

2. Diesel Governor and Its Characteristics

Inherently, a diesel generator (DG) is an unstable electromechanical machine that requires a proper control system for its operation [26]. With respect to their usage in electromechanical electrical power systems, DG units have three major components [27]:

- Automatic Voltage Regulator (AVR).
- Synchronous Generator.
- Prime Mover (PM) (in combination with Speed Governor).

In this paper, the primary topic of interest is the DG PM. The other components of a DG are outside of the scope of this paper. Therefore, the time-domain behavior model of a diesel governor has been taken from [18,28]. A diesel engine PM schematic block representation and MATLAB Simulink 2022a model are shown in Figures 1 and 2, respectively. They clearly show that a diesel PM further decomposes into several submodels, which are briefly described in the following subsections.

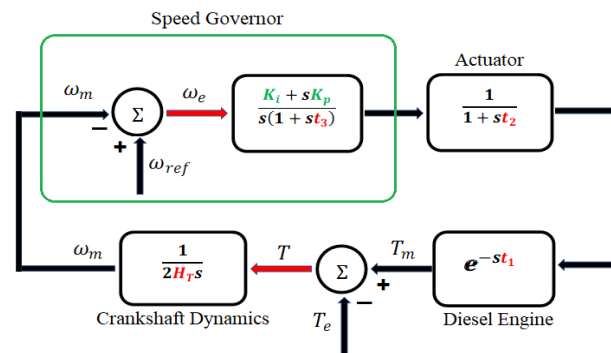


Figure 1. Schematic block representation of a diesel generator PM.

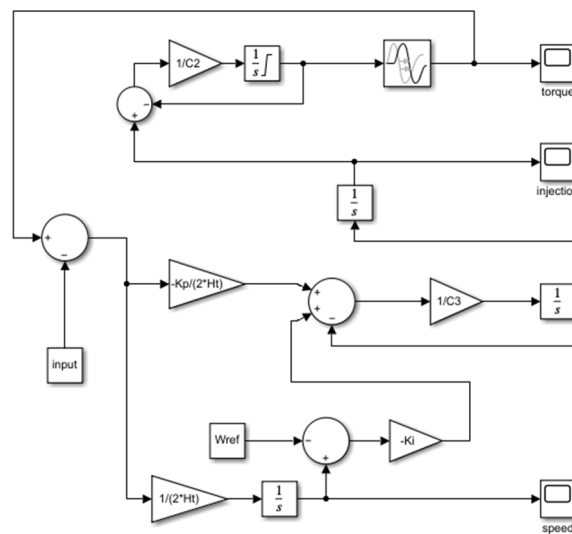


Figure 2. MATLAB Simulink 2022a representation of a diesel generator PM model.

2.1. Speed Governor (SG)

The role of a DG speed governor is to control the diesel engine speed actuating on the incoming fuel rate. Increasing or decreasing this fuel rate increases or decreases the mechanical power applied to the shaft [2]. Figure 1 shows that the SG is a combination of a filter, with the time constant t_3 , and a simple proportional integral (PI) controller with the control gains K_p and K_i . It is fed with the speed error signal, ω_e (p.u.), as described in (1).

$$\omega_e = \omega_{ref} - \omega_m. \tag{1}$$

2.2. Actuator

Its main role is to control the fuel flow into the PM. In other words, control of the fuel rack position (FRP) corresponds to the applied fuel injection rate (FIR). Here, in Figure 1, t_2 is the first-order transfer function time constant, or the actuator time constant, responsible for the delay between the FRP and FIR.

2.3. Diesel Engine (DE)

The DE, also known as the transportation delay or combustion system, as shown in block e^{-st_1} in Figure 1, is responsible for the conversion of fuel energy into shaft mechanical energy. The output of the DE corresponds to the mechanical torque T_m .

2.4. Crankshaft Dynamics (CD)

The CD in a diesel PM describe the conversion of the reciprocal motion of the piston into rotatory motion, as shown in Figure 1. Here, H_T is the inertia constant and T_e is the

torque opposed by the electrical generator. The differential equations that describe the PM of the diesel generator shown in Figures 1 and 2 are given in Equations (2)–(6).

$$\dot{x}_1 = \dot{T}_m = \left[\frac{-2t_2 - t_1}{t_1 t_2} \right] T_m + x_2 + \left(\frac{-i}{t_2} \right) \tag{2}$$

$$\dot{x}_2 = \frac{-T_m}{t_1 t_2} + \frac{2i}{t_1 t_2} \tag{3}$$

$$\dot{x}_3 = \dot{i} = \frac{-i}{t_3} + x_4 - \frac{K_p \omega_m}{t_3} + \frac{K_p \omega_{ref}}{t_3} \tag{4}$$

$$\dot{x}_4 = -\omega_m \frac{K_i}{t_3} + \frac{K_i}{t_3} \omega_{ref} \tag{5}$$

$$\dot{x}_5 = \dot{\omega}_m = \frac{1}{2H_T} (T_m - T_e) \tag{6}$$

The transportation delay is considered through its first-order Padé approximation, as shown in Equation (7).

$$e^{-st_1} = \frac{1 - \frac{t_1 s}{2}}{1 + \frac{t_1 s}{2}} \tag{7}$$

This approximation has also been applied in the calculation of the dynamic matrix corresponding to the differential Equations (2)–(6):

$$\begin{vmatrix} \frac{-2t_2 - t_1}{t_1 t_2} & 1 & \frac{-1}{t_2} & 0 & 0 \\ \frac{-1}{t_1 t_2} & 0 & \frac{2}{t_1 t_2} & 0 & 0 \\ 0 & 0 & -\frac{1}{t_3} & 1 & \frac{-K_p}{t_3} \\ 0 & 0 & 0 & 0 & \frac{-K_i}{t_3} \\ \frac{1}{2H_T} & 0 & 0 & 0 & 0 \end{vmatrix} \tag{8}$$

The characteristic polynomial of this matrix is shown in Equation (9). It is useful in the calculation of the upper limits of the controller gain parameters.

$$\lambda^5 + \frac{(t_1 t_2 + t_1 t_3 + 2t_2 t_3) \lambda^4}{t_1 t_2 t_3} + \frac{(t_1 + 2t_2 + t_3) \lambda^3}{t_1 t_2 t_3} + \frac{(-K_p t_1 + 2H_T) \lambda^2}{2H_T t_1 t_2 t_3} - \frac{(K_i t_1 - 2K_p) \lambda}{2t_1 t_2 t_3 H_T} + \frac{K_i}{t_1 t_2 t_3 H_T} = 0 \tag{9}$$

3. Materials and Methods

The proposed methodology for tuning the DG speed governor parameters is as follows.

The speed response to three different torque perturbations from the electrical generator (a step, a ramp, and a random fluctuation) is simulated during a given time period (t_{sim}) for different combinations of controller constants (K_p and K_i). These perturbations practically reflect the real-world power system scenarios, considering that they can be described as a combination of these perturbations. A step response can reflect the sudden loss of a wind generator in a hybrid power system (or the switching on of a big load). Similarly, a ramp response represents a steady wind power decrease, while a random fluctuation reflects wind, or load, variations. It is important to note that this paper focuses on diesel power plant governor tuning and tests its performance under different real-world wind variation scenarios. The performance of every combination of PI controller gains is evaluated according to different metrics: the maximum frequency error, the integral absolute error (IAE), and the integral square error (ISE). In addition, the number of differential speed sign changes (positive and negative fluctuations during a transient period) is considered.

The mathematical expressions that calculate the above-mentioned objective functions are given in Equations (10) and (11).

$$ISE = \int_0^{t_{sim}} \omega_e(t)^2 dt \quad (10)$$

$$IAE = \int_0^{t_{sim}} |\omega_e(t)| dt \quad (11)$$

Based on these objective functions, we propose the use of the Student Psychology-Based Algorithm (SPBA) for calculating the best tuning parameters of a diesel PM. Many approaches proposed in relation to the control of modern power systems are based on the natural behavior of animals, plants, insects, etc. These nature-inspired algorithms include the bat algorithm [29], harmony search [30,31], tabu search [32], genetic algorithm (based on Darwin's theory of evolution) [33], partial swarm optimization [34], grey wolf optimization [35], GA-fuzzy [36], GA-PSO [37], etc. All these algorithms have their own importance in the world of power systems and other related fields. However, we believe that some gaps remain when adopting these algorithms because the accuracy in terms of predicting the natural behavior of living things has certain uncertainties, such as human error, instrument error, environmental effects, the way of implementing a certain technique or the selection of certain variables for developing algorithms. In addition, factors such as convergence mobility and optimization play a leading role in the adaptation of the SPBA approach. This is why many references in the literature conclude that the SPBA approach, as compared to these algorithms, is superior and more effective [38–42].

The proposed SPBA approach for calculating the optimum tuning parameters of a diesel PM is based on the following objective functions: the IAE, ISE and number of output sign changes. These values are calculated for different distinctive combinations of K_p and K_i . The upper and lower limits of both gain parameters are found using Equation (9).

The SPBA-based flow chart is shown in Figure 3. This algorithm is used to find a unique optimum combination of controller gain parameters using quality performance indices (ISE and IAE) to enhance the system performance during uncertainty. To pursue this aim, we firstly evaluate the reference controller quality index, Z_{base} (Equation (12)), based on the reference model [18] controller gain parameters, i.e., K_{p_base} and K_{d_base} . In the current scenario, there are two gain parameters. Therefore, there are a maximum of eight different prospects to follow in finding the optimum values of the gain parameters. This is why the controller quality indices for all the possible scenarios are calculated by varying the values of K_{p_base} and K_{d_base} by "one" according to the applied conditions. The greater the value of the controller quality index, Z , the better the controller performance. This is why we individually compare the eight different controller quality indices with Z_{base} . In each case, there are two possibilities: either the calculated quality index is greater or lesser than Z_{base} . In the latter case, the SPBA generates zero. However, in the former case, the respective controller quality index (e.g., Z_{b_new} , Z_{c_new} , etc.) maintains its original value. All the possible results are stored in the vector \mathbf{Y} shown in Figure 3. If \mathbf{Y} is a non-zero vector, each column of \mathbf{Y} is compared with each other column to find the greatest Z . Now, the new reference controller quality index is that greatest Z , which we use to compare the next loop quality indices. This variation (=1) in the values of the gain parameters stops when $\mathbf{Y} = [0]$. In case of a null vector, the gain parameters' variation is further applied up to the first decimal place. Whenever \mathbf{Y} is equal to a null vector, it means that the gain parameters against Z_{prev} are in an optimum position against the respective variation in K_{p_base} and K_{d_base} . In this paper, the optimum values of K_p and K_d up to the second decimal place are provided. Beyond the second decimal place, the variation in the gain parameters shows no significant improvement in the values of Z and $NADIR$. This means that the third time $\mathbf{Y} = [0]$, the algorithm stops and generates optimum results for the current controller. The main benefit of this SPBA approach is that the system remains stable, because every simulation moves the controller gain parameters toward the optimum stability region. The optimum result reflects the combined effects of the minimum ISE, IAE and number

of fluctuations for a specific controller. The effectiveness of this proposed approach is discussed in detail in the following case study.

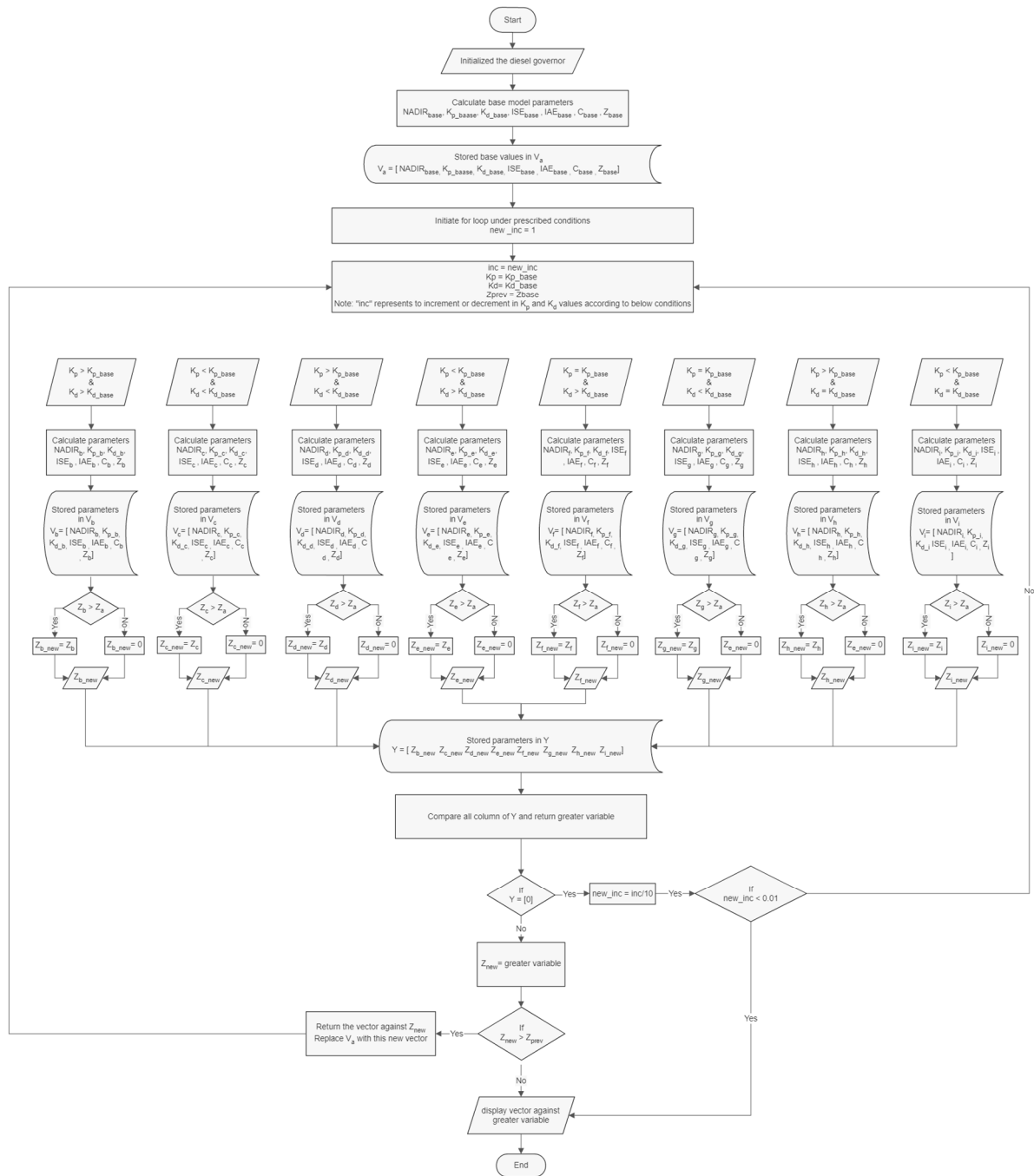


Figure 3. Flow chart of the SPBA for tuning the controller gain parameters.

4. Case Study

To illustrate the application of the proposed methodology, a case study conducted on San Cristobal Island, Galapagos Archipelago, Ecuador, is presented in this section. Its power system has a diesel power plant with three diesel generators of 813 kVA and 650 kW [18]. The detailed diesel generator specification is shown in Table 1. It is observed that the WDPS of San Cristobal Island faces frequency deviation problems. Therefore, the San Cristobal hybrid WDPS attracts researchers’ attention and requires specific treatment to mitigate these power frequency problems, which may affect the power plant’s reliability

in the most severe wind conditions. To reduce the frequency deviation problems in such hybrid power plants, the controller of the DG PM plays a key role in the power system's operation. Correspondingly, the DG PM controller performance depends directly on controller gains tuning, such as K_p and K_i .

Table 1. Dataset of the DPS installed on San Cristobal Island [18].

Model of diesel engine	CAT-3512 DITA
Rated frequency	60 Hz
Synchronous speed	1200 rpm
Capacity	813 kVA
Rated power	650 kW
Constant of inertia (H_T)	0.4208 s
Output voltage	480 V \pm 5%
Time constants: t_1, t_2, t_3	0.024 s, 0.1 s, 0.01 s
Maximum torque (T_{max}), minimum torque (T_{min})	1.1 p.u., 0 p.u.

The proposed approach seeks the best combination of PI controller gain parameters that provide the minimum IAE and ISE values, as described in the previous section. After testing and evaluating the results of thousands of combinations, the SPBA (Figure 3) has found that the best controller gain parameters for the San Cristobal Island case are $K_p = 10.13$ and $K_i = 13.35$. If we increase or decrease the values of K_p and K_i from the proposed optimum values, then the system behavior tends toward being worse in terms of increased oscillations, increased settling time and frequency deviation. Therefore, to validate the proposed tuning parameters, three different perturbations (step, ramp and random) are considered as torque inputs for the power controller, and the simulation results are compared with those corresponding to the Ochoa and Martinez controller parameters [18]. The simulation results show that the proposed control parameters provide a better response, showing less frequency deviation and better system stability. Detailed discussions concerning the simulations and results are presented in Section 5.

5. Results

This section presents the detailed simulation results of the San Cristobal Island case study and compares the behavior of the system with two different controllers: the one obtained with the proposed methodology and the one proposed in [18] as a benchmark.

5.1. Step Response

A step variation in the electric generator torque is applied as an input to the system. Figure 4 shows significant differences between the speed responses of the two controllers: the benchmark and the proposed one. The system response with the proposed gain parameters shows superior and more efficient behavior. In this case, the system is stable or maintains a constant speed of 1 p.u. after 2 s, as compared to the benchmark [18], which needs 15.3 s to stabilize the system.

In addition, the values of the integral square error and integral absolute error of both controllers are shown in Table 2. Similarly, during transients, the minimum underfrequency is reduced by 3.006 Hz (58.548 Hz versus 55.542 Hz). In other words, the frequency during transients is closer to the system rated frequency (60 Hz).

As a metric of the controller effectiveness, a control quality index "Z" is introduced. It estimates the controller performance based on the minimum underfrequency, ISE, IAE and the number of sign changes in the frequency derivative during transients, as defined in Equation (12), where v represents the minimum speed, or underfrequency, and c is the number of sign changes in the speed derivative during the disturbance.

$$Z = \frac{v}{ISE \cdot IAE \cdot c} \quad (12)$$

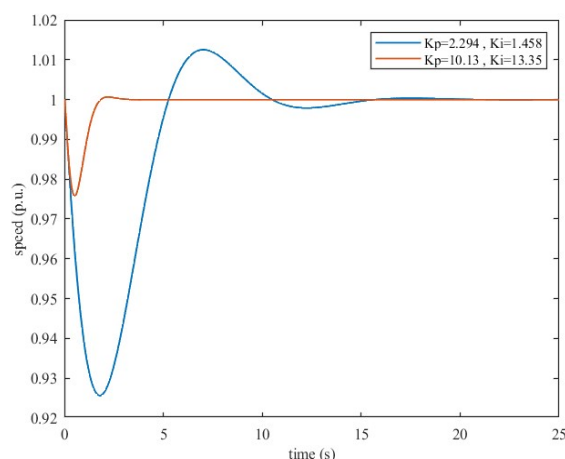


Figure 4. Speed response to an electrical torque step.

Table 2. Comparison of the control performance metrics with different gain parameters following a step input.

	Benchmark [18]: $K_p = 2.294$ and $K_i = 1.458$	Proposed Methodology: $K_p = 10.13$ and $K_i = 13.35$
Minimum speed (p.u.)	0.9257	0.9758
ISE (p.u.)	0.2175	0.2045
IAE (p.u.)	0.4793	0.2265
Control quality index "Z"	2.2199	10.5334
Minimum frequency (Hz)	55.542	58.548

The control quality index is used as a reference parameter when the performance of several controllers is compared. The higher the value of v , the better the performance of the controller, i.e., the controller performance is better if the minimum underfrequency is higher. In addition, the performance is better if the ISE and IAE are lower. To reduce the engine valves' effort (and, consequently, their wear and tear), it is convenient to reduce the number of derivative sign changes. Thus, the Z index is proportional to the minimum underfrequency and inversely proportional to the product of the ISE, IAE and c .

5.2. Ramp Response

When using an electric torque ramp as an input to the system, its behavior with the controller gains obtained with the proposed tuning methodology is also satisfactory, as can be seen in Figure 5. It shows that the minimum speed during transients is up to 0.9915 p.u., a little frequency deviation when compared to the one obtained with the benchmark [18]. In addition, a reduction in the area under the curve during transients is achieved. Similarly, the frequency response is improved by 4.188 Hz (59.49 Hz versus 55.302 Hz). Moreover, the power system becomes stable after 6 s with the proposed tuning versus 20 s with the benchmark. Additional metrics can be seen in Table 3.

Table 3. Comparison of the control performance metrics with different gain parameters following a ramp input.

	Benchmark [18]: $K_p = 2.294$ and $K_i = 1.458$	Proposed Methodology: $K_p = 10.13$ and $K_i = 13.35$
Minimum speed (p.u.)	0.9217	0.9915
ISE (p.u.)	0.2225	0.2044
IAE (p.u.)	0.5902	0.2478
Control quality index "Z"	1.4037	6.5251
Minimum frequency (Hz)	55.302	59.49

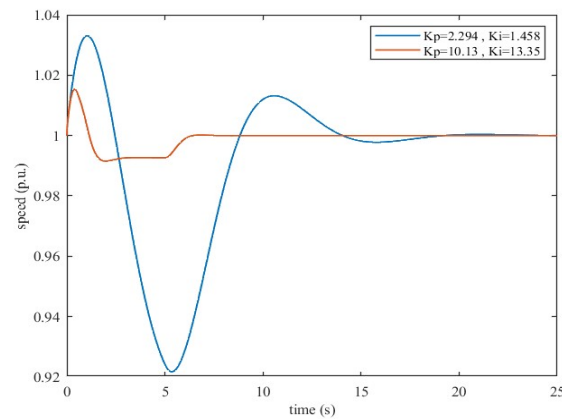


Figure 5. Speed response to an electrical torque ramp.

5.3. Response to a Random Input

As previously stated, to validate the controller’s adequacy for real-world power systems, an additional assessment of its behavior against random disturbances or noise is needed. The system response to the random torque input shown in Figure 6 is tested. Regarding the speed response, it is observed that the controller performance is smoother with the proposed gain parameters, as shown in Figure 7. Furthermore, the absolute error is much lower than the one obtained with Ochoa and Martinez [18] tuning. Table 4 summarizes the main quality response metrics.

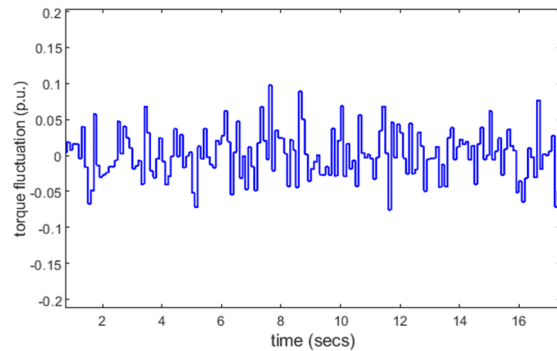


Figure 6. Electrical torque random input considered.

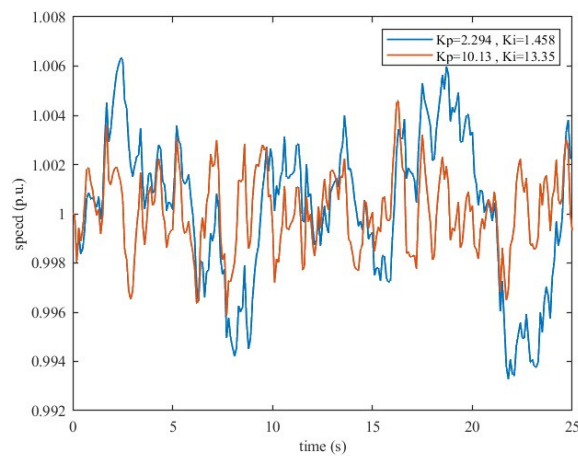


Figure 7. Speed response to a random electrical torque.

Table 4. Comparison of the control performance metrics with different gain parameters following a random input.

	Benchmark [18]: $K_p = 2.294$ and $K_i = 1.458$	Proposed Methodology: $K_p = 10.13$ and $K_i = 13.35$
ISE (p.u.)	0.2043	0.2041
IAE (p.u.)	0.2648	0.2355

6. Conclusions

In this paper, an SPBA-based tuning methodology for diesel engine governors is proposed. The main advantage of this proposed approach is providing a unique optimum combination of controller gain parameters. If we increased or decreased the values of the gain parameters from the proposed optimum values, then the system behavior tended toward being worse in terms of increased oscillations, increased settling time and frequency deviation. To test its effectiveness, it has been applied to the tuning of the WDPS on San Cristobal Island. The simulated response exhibits an enhancement versus the original tuning of this governor. In particular, three types of perturbations (step, ramp, and random electrical torque inputs) that reflect the sudden loss of a wind generator, a steady wind power decrease and wind variations, respectively, were considered. The quality of the response was evaluated via calculation of several performance indices: the ISE, IAE and the proposed index Z . Based on these indices, control gain parameters that reduce the power system frequency deviation were obtained. Regarding these control factors, the system shows better behavior for the IAE: with the obtained control parameters, the IAE is reduced by 52%, 58% and 11% in response to step, ramp, and random electrical torque perturbations, respectively. Furthermore, the maximum frequency deviation is reduced by 5.3% and 7.6% against step and ramp perturbations, as compared to the original response of the San Cristobal WDPS tuning. In summary, the simulation results show the usefulness of the proposed tuning methodology.

Author Contributions: Conceptualization, J.A.S.-F. and S.M.; methodology, J.A.S.-F. and M.A.; software, M.A. and J.A.S.-F.; validation, M.A. and J.A.S.-F.; formal analysis, M.A. and J.A.S.-F.; investigation, M.A. and J.A.S.-F.; resources, J.A.S.-F. and S.M.; data curation, M.A. and J.A.S.-F.; writing—original draft preparation, M.A. and J.A.S.-F.; writing—review and editing, S.M. and J.A.S.-F.; visualization, M.A. and J.A.S.-F.; supervision, J.A.S.-F. and S.M.; project administration, J.A.S.-F. and S.M.; funding acquisition, S.M. and J.A.S.-F. All authors have read and agreed to the published version of the manuscript.

Funding: This work was supported by the Spanish National Research Agency “Agencia Estatal de Investigación” under grant number PID2019-108966RB-I00/AEI/10.13039/501100011033.

Data Availability Statement: All the data supporting the reported results can be found in this paper and in the cited references.

Conflicts of Interest: The authors declare no conflict of interest. The funders had no role in the design of the study; in the collection, analysis, or interpretation of the data; in the writing of the manuscript; or in the decision to publish the results.

References

- Lu, J.; Wang, W.; Zhang, Y.; Cheng, S. Multi-Objective Optimal Design of Stand-Alone Hybrid Energy System Using Entropy Weight Method Based on HOMER. *Energies* **2017**, *10*, 1664. [[CrossRef](#)]
- Sebastian, R.; Garcia-Loro, F. Review on Wind Diesel Systems Dynamic Simulation. In Proceedings of the 45th Annual Conference of the IEEE Industrial Electronics Society, Lisbon, Portugal, 14–17 October 2019. [[CrossRef](#)]
- Barasa Kabeyi, M.J.; Olanrewaju, O.A. Geothermal wellhead technology power plants in grid electricity generation: A review. *Energy Strategy Rev.* **2022**, *39*, 100735. [[CrossRef](#)]
- Asad, M. Improving Power Flow Using Static Synchronous Series Compensator. *Egypt. J. Eng. Sci. Technol.* **2021**, *33*, 69–74. [[CrossRef](#)]
- Martínez-Lucas, G.; Sarasúa, J.I.; Sánchez-Fernández, J.Á.; Wilhelmi, J.R. Frequency control support of a wind-solar isolated system by a hydropower plant with long tail-race tunnel. *Renew. Energy* **2016**, *90*, 362–376. [[CrossRef](#)]

6. Erdiwansyah; Mamat, R.; Sani, M.S.M.; Sudhakar, K. Renewable energy in Southeast Asia: Policies and recommendations. *Sci. Total Environ.* **2019**, *670*, 1095–1102. [[CrossRef](#)] [[PubMed](#)]
7. Martínez-Lucas, G.; Sarasúa, J.I.; Sánchez-Fernández, J.Á. Eigen analysis of wind–hydro joint frequency regulation in an isolated power system. *Int. J. Electr. Power Energy Syst.* **2018**, *103*, 511–524. [[CrossRef](#)]
8. Abdulkarim, A.; Faruk, N.; Oloyode, A.O.; Olawoyin, L.A.; Popoola, S.I.; Abdullateef, A.I.; Ibrahim, O.; Surajudeen-Bakinde, N.T.; Abdelkader, S.M.; Morrow, J.D.; et al. State of the Art in Research on Optimum Design, Reliability and Control of Renewable Energy Microgrids. *ELEKTRIKA-J. Electr. Eng.* **2018**, *17*, 23–35. [[CrossRef](#)]
9. Bueno, C.; Carta, J.A. Wind Powered Pumped Hydro Storage Systems, a Means of Increasing the Penetration of Renewable Energy in the Canary Islands. *Renew. Sustain. Energy Rev.* **2006**, *10*, 312–340. [[CrossRef](#)]
10. Kaldellis, J.K.; Kavadias, K.; Christinakis, E. Evaluation of the Wind–Hydro Energy Solution for Remote Islands. *Energy Convers. Manag.* **2001**, *42*, 1105–1120. [[CrossRef](#)]
11. Vasconcelos, H.; Moreira, C.; Madureira, A.; Lopes, J.P.; Miranda, V. Advanced Control Solutions for Operating Isolated Power Systems: Examining the Portuguese Islands. *IEEE Electr. Mag.* **2015**, *3*, 25–35. [[CrossRef](#)]
12. Arévalo, P.; Eras-Almeida, A.A.; Cano, A.; Jurado, F.; Egidio-Aguilera, M.A. Planning of Electrical Energy for the Galapagos Islands Using Different Renewable Energy Technologies. *Electr. Power Syst. Res.* **2022**, *203*, 107660. [[CrossRef](#)]
13. Icaza-Alvarez, D.; Jurado, F.; Tostado-Véliz, M.; Arevalo, P. Decarbonization of the Galapagos Islands. Proposal to Transform the Energy System into 100% Renewable by 2050. *Renew. Energy* **2022**, *189*, 199–220. [[CrossRef](#)]
14. Ye, B.; Zhang, K.; Jiang, J.; Miao, L.; Li, J. Towards a 90% Renewable Energy Future: A Case Study of an Island in the South China Sea. *Energy Convers. Manag.* **2017**, *142*, 28–41. [[CrossRef](#)]
15. Ren, G.; Liu, J.; Wan, J.; Guo, Y.; Yu, D. Overview of wind power intermittency: Impacts, measurements, and mitigation solutions. *Appl. Energy* **2017**, *204*, 47–65. [[CrossRef](#)]
16. Rashid, G.; Lone, S.A.; Mufti, M.U.-D. Modeling and Performance Assessment of an Isolated Wind-Diesel System with Flywheel Energy Storage System. *Wind Eng.* **2023**, *47*, 597–606. [[CrossRef](#)]
17. Sebastián, R. Application of a Battery Energy Storage for Frequency Regulation and Peak Shaving in a Wind Diesel Power System. *IET Gener. Transm. Distrib.* **2016**, *10*, 764–770. [[CrossRef](#)]
18. Ochoa, D.; Martinez, S. Proposals for Enhancing Frequency Control in Weak and Isolated Power Systems: Application to the Wind-Diesel Power System of San Cristobal Island-Ecuador. *Energies* **2018**, *11*, 910. [[CrossRef](#)]
19. Elistratov, V.; Konishchev, M.; Denisov, R.; Bogun, I.; Grönman, A.; Turunen-Saaresti, T.; Lugo, A.J. Study of the Intelligent Control and Modes of the Arctic-Adopted Wind–Diesel Hybrid System. *Energies* **2021**, *14*, 4188. [[CrossRef](#)]
20. Kharrich, M.; Kamel, S.; Abdeen, M.; Mohammed, O.H.; Akherraz, M.; Khurshaid, T.; Rhee, S.B. Developed approach based on equilibrium optimizer for optimal design of hybrid PV/Wind/Diesel/Battery Microgrid in Dakhla, Morocco. *IEEE Access* **2021**, *9*, 13655–13670. [[CrossRef](#)]
21. Kaldellis, J.K.; Kavadias, K.A. Cost-benefit analysis of remote hybrid wind-diesel power stations: Case study Aegean Sea islands. *Energy Policy* **2007**, *35*, 1525–1538. [[CrossRef](#)]
22. Nguyen-Hong, N.; Nguyen-Duc, H.; Nakanishi, Y. Optimal Sizing of Energy Storage Devices in Isolated Wind-Diesel Systems Considering Load Growth Uncertainty. *IEEE Trans. Ind. Appl.* **2018**, *54*, 1983–1991. [[CrossRef](#)]
23. El-Bidairi, K.S.; Nguyen, H.D.; Mahmoud, T.S.; Jayasinghe, S.D.G.; Guerrero, J.M. Optimal sizing of Battery Energy Storage Systems for dynamic frequency control in an islanded microgrid: A case study of Flinders Island, Australia. *Energy* **2020**, *195*, 117059. [[CrossRef](#)]
24. Dorf, R.; Bishop, R. *Modern Control Systems*, 13th ed.; Pearson: London, UK, 2016; ISBN 978-0134407623.
25. Gonzales-Zurita, O.; Andino, O.L.; Clairand, J.-M.; Escrivá-Escrivá, G. PSO Tuning of a Second-Order Sliding Mode Controller for Adjusting Active Standard Power Levels for Smart Inverter Applications. *IEEE Trans. Smart Grid* **2023**, *1*. [[CrossRef](#)]
26. Sinha, R.P.; Balaji, R. A Mathematical Model of Marine Diesel Engine Speed Control System. *J. Inst. Eng.* **2018**, *99*, 63–70. [[CrossRef](#)]
27. Theubou, T.; Wamkeue, R.; Kamwa, I. Dynamic model of diesel generator set for hybrid wind-diesel small grids applications. In Proceedings of the 25th IEEE Canadian Conference on Electrical and Computer Engineering, Montreal, QC, Canada, 29 April–2 May 2012. [[CrossRef](#)]
28. Sharaf, A.M.; Abdin, E.S. A digital simulation model for wind-diesel conversion scheme. In Proceedings of the Twenty-First Southeastern Symposium on System Theory, Tallahassee, FL, USA, 26–28 March 1989. [[CrossRef](#)]
29. Yang, X.S. Bat algorithm for multi-objective optimization. *Int. J. Bio-Inspired Comput.* **2011**, *3*, 267–274. [[CrossRef](#)]
30. Lee, K.S.; Geem, Z.W. A new meta-heuristic algorithm for continuous engineering optimization: Harmony search theory and practice. *Comput. Methods Appl. Mech. Eng.* **2005**, *194*, 3902–3933. [[CrossRef](#)]
31. Das, S.; Mukhopadhyay, A.; Roy, A.; Abraham, A.; Panigrahi, B.K. Exploratory Power of the Harmony Search Algorithm: Analysis and Improvements for Global Numerical Optimization. *IEEE Trans. Syst. Man Cybern.* **2011**, *41*, 89–106. [[CrossRef](#)]
32. Glover, F. Tabu Search—Part I. *ORSA J. Comput.* **1989**, *1*, 190–206. [[CrossRef](#)]
33. Holland, J.H. *Adaptation in Natural and Artificial Systems: An Introductory Analysis with Applications to Biology, Control, and Artificial Intelligence*; The MIT Press: Cambridge, MA, USA, 1992. [[CrossRef](#)]
34. Kennedy, J.; Eberhart, R. Particle swarm optimization. In Proceedings of the ICNN'95—International Conference on Neural Networks, Perth, WA, Australia, 27 November–1 December 1995. [[CrossRef](#)]

35. Mirjalili, S.; Mirjalili, S.M.; Lewis, A. Grey Wolf Optimizer. *Adv. Eng. Softw.* **2014**, *69*, 46–61. [[CrossRef](#)]
36. Hsiao, Y.-T.; Chen, C.-H.; Chien, C.-C. Optimal capacitor placement in distribution systems using a combination fuzzy-GA method. *Int. J. Electr. Power Energy Syst.* **2004**, *26*, 501–508. [[CrossRef](#)]
37. Kao, Y.-T.; Zahara, E. A hybrid genetic algorithm and particle swarm optimization for multimodal functions. *Appl. Soft Comput.* **2008**, *8*, 849–857. [[CrossRef](#)]
38. Das, B.; Mukherjee, V.; Das, D. Student psychology based optimization algorithm: A new population based optimization algorithm for solving optimization problems. *Adv. Eng. Softw.* **2020**, *146*, 102804. [[CrossRef](#)]
39. Mudi, J.; Shiva, C.K.; Mukherjee, V. An Optimal Control of Integrated Hybrid Power System with FACTS Devices Using Student Psychology-Based Optimization Algorithm. *Adv. Theory Simul.* **2021**, *4*, 2100147. [[CrossRef](#)]
40. Das, M.K.; Bera, P.; Sarkar, P.; Chakrabarty, K. PI-RLNN Controller for LFC of Hybrid Deregulated Power System Based on SPOA. In Proceedings of the IEEE 18th India Council International Conference, Guwahati, India, 19–21 December 2021. [[CrossRef](#)]
41. Das, B.; SoumyabrataBarik; Das, D.; Mukherjee, V. Optimization Algorithm for Renewable Energy Integration. In *Intelligent Renewable Energy Systems*; Priyadarshi, N., Bhoi, A.K., Padmanaban, S., Balamurugan, S., Holm-Nielsen, J.B., Eds.; John Wiley & Sons, Inc.: Hoboken, NJ, USA, 2022; Chapter 1; pp. 1–39. [[CrossRef](#)]
42. Kalman, R.E. Design of a Self-Optimizing Control System. *Trans. Am. Soc. Mech. Eng.* **1958**, *80*, 468–477. [[CrossRef](#)]

Disclaimer/Publisher’s Note: The statements, opinions and data contained in all publications are solely those of the individual author(s) and contributor(s) and not of MDPI and/or the editor(s). MDPI and/or the editor(s) disclaim responsibility for any injury to people or property resulting from any ideas, methods, instructions or products referred to in the content.